Atomization and Sprays, 23 (6): 505–515 (2013)

HIGH RESOLUTION OPTICAL EXPERIMENTAL TECHNIQUE FOR COMPUTING PULSED LASER-INDUCED CAVITATION BUBBLE DYNAMICS IN A SINGLE SHOT

Luis Felipe Devia-Cruz,[1,*] Francisco G. Pérez-Gutiérrez,[2] Daniel García-Casillas,[3] Guillermo Aguilar,[3] Santiago Camacho-López,[1] & Darren Banks[3]

[1] *Departamento de Óptica, Centro de Investigación Científica y de Educación Superior de Ensenada, Mexico*

[2] *Facultad de Ingeniería, Universidad Autónoma de San Luis Potosí, Mexico*

[3] *Department of Mechanical Engineering, University of California, Riverside, California, USA*

[*] Address all correspondence to Luis Felipe Devia-Cruz
E-mail: ldevia@cicese.edu.mx

Original Manuscript Submitted: 02/04/2013; Final Draft Received: 03/14/2013

The experiments conducted in this study consisted of a series of plasma generated cavitation bubbles in water, obtained by focusing a 532-nm Q-switched Nd:YAG nanosecond-pulsed laser. For the purpose of detection of such cavitation bubbles, a novel direct light transmission technique is used, referred to as spatial transmission modulation (STM), consisting of a nearly collimated beam of light passing through the sample at the point where the cavitation bubble is formed. The presence of the cavitation bubble modifies the direct light transmission, which is detected with a photodiode located at the opposite end. This is observed as an electrical signal response with an oscilloscope. A 1-megapixel high-speed video camera simultaneously records the cavitation event. The video was taken in an orthogonal direction with respect to the STM optical axis and was triggered simultaneously with an oscilloscope using the electronic synchronization signal from the pulsed laser. Data from the high-speed video was used to show that a computational spatial energetic analysis from the continuous laser probe beam is a valid method to directly obtain the cavitation bubble evolution from a single shot pulse.

KEY WORDS: *cavitation, pulsed laser, plasma*

1. INTRODUCTION

Cavitation is an interesting mechanical phenomenon from a thermodynamic point of view due to its complexity, and it has been a subject of study in some fundamental and applied fields such as the damage caused in turbines and propellers (Vogel et al., 1989), and medical areas such as ophthalmology (Oraevsky et al., 1996). With the use of Q-switched lasers, a new way to induce the cavitation process was created: laser mediated cavitation.

The laser mediated cavitation is generated in liquids starting from a laser-induced dielectric breakdown resulting in a plasma formation. This process also involves an avalanche ionization effect and Coulomb repulsion forces, which produce strong and very fast mechanical expansions, generating two main phenomena: shock wave fronts and cavitation bubbles (Vogel and Lauterborn, 1988). The cavitation bubble grows to a maximum size and then collapses to generate another bubble; this bouncing behavior occurs for several subsequent bubbles (Evans and Camacho-López, 2010), and each collapse is related to the generation of a spherical shock wave front (Vogel and Lauterborn, 1988). The shock wave is considered the principal mechanism for mechanical damage associated with cavitation (Kaustubh et al., 2006). The subsequent bubbles have a smaller size than the first one because of the dissipation of mechanical energy due to viscous effects.

Several techniques have been widely used to study such cavitation bubbles: time-resolved shadowgraphy, high-speed photography (Lauterborn and Ohl, 1997), streak photography (Docchio et al., 1988), interferometry (Pérez-Gutiérrez et al., 2011), opto-acoustic detection (Oraevsky et al., 1995) and optical beam deflection (Petkovsek et al., 2007; Gregorčič et al., 2008).

Until recently, high-speed video (up to 75,000 frames per second) techniques have not been fast enough to resolve cavitation bubble dynamics and detect accurately the exact instant of the bubble collapse. Since the photographic methods are discrete, i.e., there is a relatively "long period of time" between each image, important stages of the cavitation event, such as the instant of collapse, can be missed. This problem has been addressed using time-resolved shadowgraphy (Evans et al., 2008), in which several time-delayed images from different independent pulse shots are combined to recreate the dynamics of an average bubble with pulse shots and time resolution on the order of nanoseconds; however, the cavitation event is typically different from shot to shot (Prentice et al., 2005), even for several shots with the same energy per pulse (which is very difficult to obtain due to quantic processes in the laser cavity), due to the stochastic nature of the laser-induced plasma. Therefore, the reconstruction of the bubble dynamics from the high-speed video and the time-resolved shadowgraphy methods is only an approximation of the real cavitation bubble behavior. In addition, the use of high-speed cameras, say over 3×10^5 fps, is very expensive and still is not always able to capture a frame with either the maximum bubble radius or the exact instant of the bubble collapse.

The optical beam deflection (OBD) technique uses a low-power continuous wave laser beam focused to irradiate a point near the bubble center, which is then collected and sent on to a photodiode. The resulting trace of the transmitted light along cavitation time extracts spatial and temporal information of both the bubble and shock wave front from a single laser pulse. This technique as published by several authors (Xu et al., 2008; Liu et al., 2010) required several exposures due to its reduced study region that is limited to the beam diameter or the beam waist.

When studying cavitation bubble dynamics, the bubble collapse time can be calculated from the maximum bubble radius using the Rayleigh-Plesset's relation, Eq. (1), below (Alehossein and Qin, 2007; Brujan and Vogel, 2006). However, this relation is not useful when the cavitation occurs close to solid boundaries. Therefore, a direct measurement method of the bubble radius (not based on collapse time) is mandatory.

$$t_c = \sqrt{\frac{3\rho}{2p_o}} \int_0^{R_{\max}} \left[\frac{(R/R_{\max})^{3/2}}{(1 - R^3/R_{\max}^3)^{1/2}} \right] dR = 0.915 R_{\max} \sqrt{\frac{\rho}{p_o}} \tag{1}$$

where $R_{\max}$ is the maximum bubble radius, R is the radius of the boundary, p_o is the liquid pressure, and ρ is the density. This work is focused on the use and improving features of the spatial transmittance modulation (STM) technique (Devia et al., 2012) which offers high resolution oscilloscope traces from the cavitation bubble geometry (radius) and its dynamics (first and second collapse times). The STM technique provides the bubble collapse time data accurately through an optical intensity vs time trace. In addition, the proposed technique provides information directly related to the bubble size, since the presence of the bubble directly affects the transmittance of a continuous probe laser beam. In this paper, we present and discuss both the aforementioned STM technique and an algorithm developed to use the STM data in order to analyze and determine the laser-induced cavitation bubble dynamics (bubble radius vs time) accurately with the data recorded from a single shot.

2. METHODOLOGY

2.1 Experimental Setup

The optical setup integrates the STM technique with high-speed video at 75,000 fps and consists of three lasers. The first one is the pump laser, a 532-nm frequency-doubled Nd:YAG (see Fig. 1) with 820 μJ ± 57 μJ energy per pulse at a 10-Hz repetition rate; the second, a red probe beam, is a 0.5-mW continuous wave laser at 633 nm; the third one, the image forming laser, is a 405-nm, violet-blue pen pointer with 4-mW output power. The output of the pump laser is reflected on a dichroic mirror and focused in the center of a quartz cuvette filled with purified water; a red laser goes through the same dichroic mirror and passes throughout the cuvette collinearly, and aligns to the center of the beam waist of the pump laser, where the bubble is formed. The transmitted beam is aligned

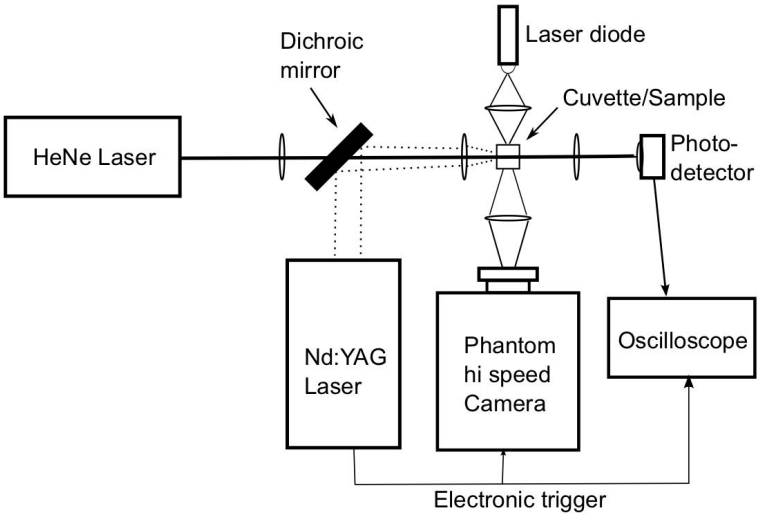

FIG. 1: Experimental setup.

to hit a photo detector located after the cuvette; the presence of the growing/collapsing bubble affects the amount of light that reaches to the photo detector (see Fig. 2), and produces an intensity trace which changes with time.

The image of the growing/collapsing bubble is formed on an orthogonal view with respect to the STM axis and is recorded with a Phantom MIRO M/LC310 camera using various resolutions and frame rates. To create these images the blue laser (405 nm) is used as the illumination source. An optical fiber tip (III) of 125 μm width is held in the frames for size reference, as seen in Fig. 3. Additional experiments with the fiber tip

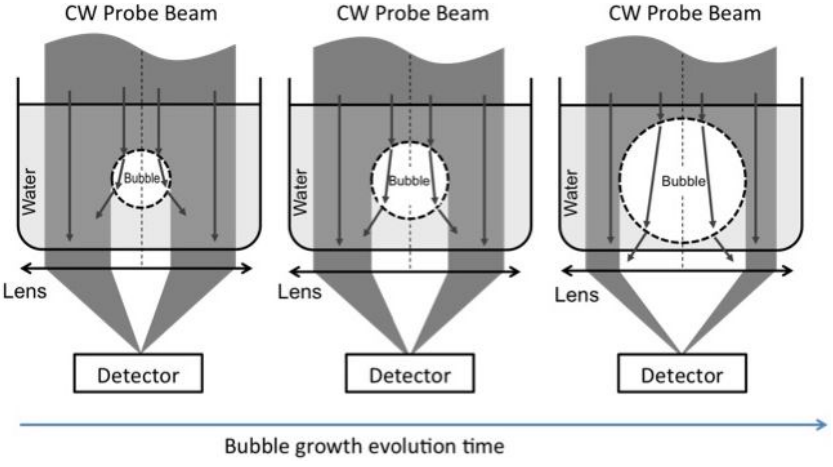

FIG. 2: Spatial transmittance modulation as observed by the growth of the cavitation bubble.

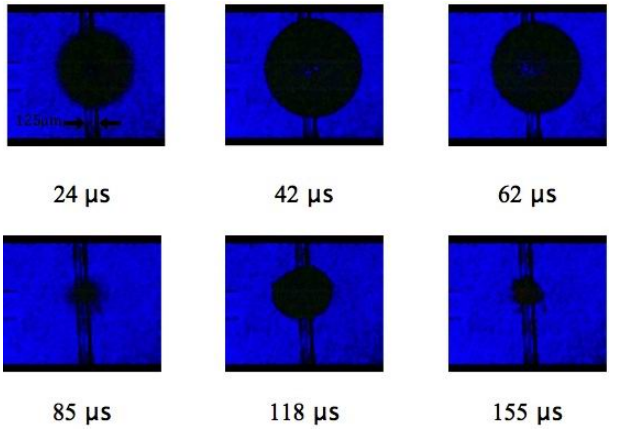

FIG. 3: Frames from high-speed video (75,000 fps) of a single shot cavitation event.

removed were carried out to prove that the fiber tip presence does not affect the bubble dynamics.

2.2 Experiments

For the purpose of this research, we conducted some experiments in which an STM optical setup was complemented by a CMOS technology sensor high-speed video camera. We synchronized the trigger from the external Q-switch electronic signal to start simultaneously both the oscilloscope and the high-speed camera.

The electrical signal recorded from the oscilloscope at a sample rate of 10×10^6 samples per second was stored as a data file for further analysis and paired with an archive of the video. The video was stored in a format that allowed us to know the exact time of the trigger relative to the recording, and to make a frame by frame comparison with the discrete time electrical signal from the oscilloscope, in such a way that allowed us to also understand qualitatively the relationship between the electrical signal detected and the behavior of the bubbles.

3. RESULTS

A typical trace from the STM technique is shown in Fig. 4. This trace shows the evolution of a cavitation bubble induced by a single laser pulse. During the expansion of the bubble the photodiode output signal decreases, coming to a minimum value when the bubble reaches its maximum size. As the bubble shrinks the signal intensity rises to a first maximum value: the first bubble collapse. Since cavitation phenomena have oscillating behavior, it undergoes several bubble expansion–collapse events. The STM technique makes the subsequent bubble collapses quite evident. We have observed as many as three well resolved collapses of bubbles produced by a single laser shot.

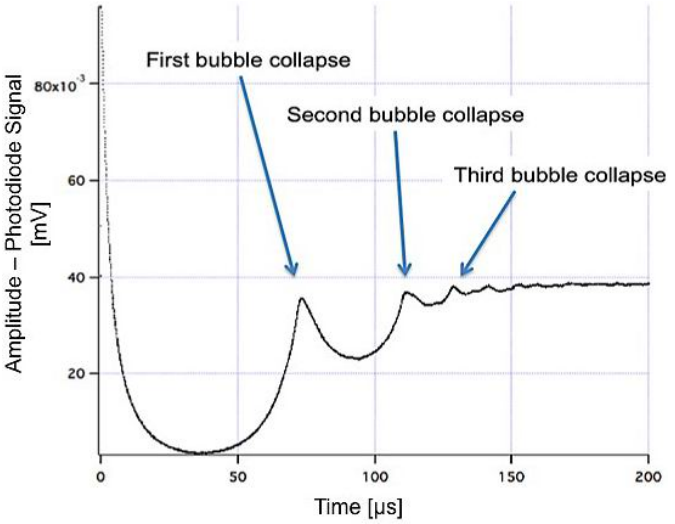

FIG. 4: Typical STM electric signal where three bubble collapses are well resolved.

The continuous line in Fig. 5 represents an experimental STM trace and the open circles represent the direct radius of the bubble measured from images taken with the high-speed camera. The recorded data from the high-speed videos at 75,000 fps fail to provide an accurate value for the collapse time nor the number of collapses. Therefore, sometimes the data from the video frames may show that there were only two collapses, while the STM signal reveals that there were actually three collapses during the whole event (i.e., one collapse occurred in between frames).

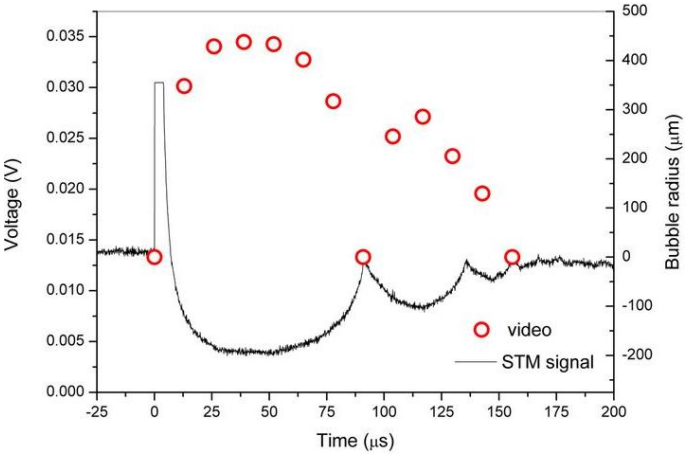

FIG. 5: Comparison of high-speed video (open circles) and STM signal (continuous line) results; note that following the trend of the open circles it appears that only two collapses occurred, while STM reveals a third collapse.

4. DISCUSSION

4.1 Theoretical Analysis of the STM Technique

The signal from the STM technique can be analyzed theoretically assuming that the He-Ne probe beam has a Gaussian TEM_{00} profile, which is partially blocked by the growing/collapsing bubble as it expands and collapses, and that the photodiode voltage signal is proportional to the integral of the intensity of such beam that is screened by the expanding and collapsing bubble according to

$$V(t) \propto \int_{-w}^{w} e^{-r^2/2w^2} dr - \int_{-R(t)}^{R(t)} e^{-r^2/2w^2} dr \tag{2}$$

where $V(t)$ is the photodiode voltage signal as a function of time, w is the He-Ne probe beam radius measured at $1/e^2$ of the maximum intensity, $R(t)$ is the bubble radius obtained from the high-speed video, and r is the radial coordinate.

In Eq. (2), the first integral is a constant and represents the area under the curve of the probe beam profile, while the second integral represents the area under the curve of the probe beam portion blocked by the bubble; the difference represents the time-dependent unblocked portion of the probe beam that is incident on the photodiode and recorded by the oscilloscope. Figure 6 shows that the calculation carried out with Eq. (2), based on bubble diameter measurements made from the accompanying video recording, matches with the experimentally obtained STM signal very accurately.

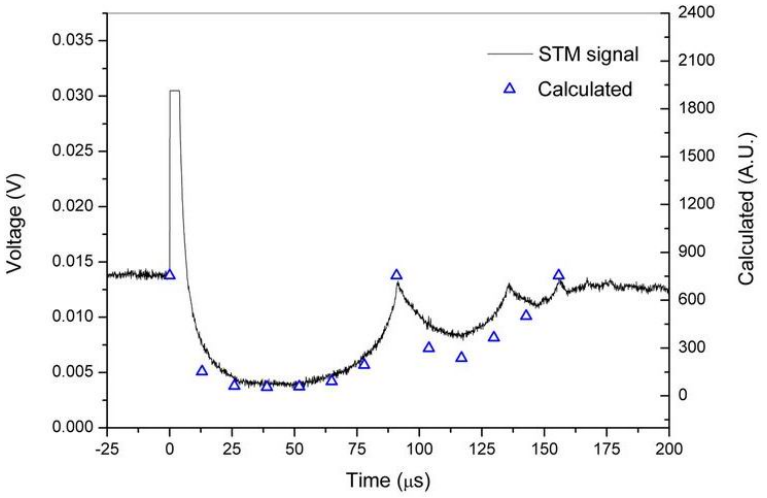

FIG. 6: Comparison of theoretical analysis of the STM signal (open triangles) with experimental results (continuous line).

4.2 Algorithm to Determine Bubble Dynamics

Once the STM technique was established theoretically, a numerical code was developed and implemented to determine the size of the bubble directly from the STM signal. Figure 7 shows the block diagram describing the algorithm. The first step is to load the oscilloscope data obtained experimentally from the STM signal (STMr) and divide each voltage point by the initial value of the data (before the pump pulse is triggered and therefore prior to bubble formation) to normalize the voltage readings against the unobstructed value; this step eliminates the peak originated by the light from the green, nanosecond, laser pump pulse that is able to pass through the filter before the photodiode. The second step is to assign a value to a test radius variable (rp), the algorithm initializes with rp = 0.001 μm. The third step is to evaluate the normalized theoretical STM signal value ($STMt$) using Eq. (3) below:

$$STMt = \frac{\int_{-w}^{w} e^{-r^2/2w^2} dr - \int_{-rp}^{rp} e^{-r^2/2w^2} dr}{\int_{-w}^{w} e^{-r^2/2w^2} dr} \tag{3}$$

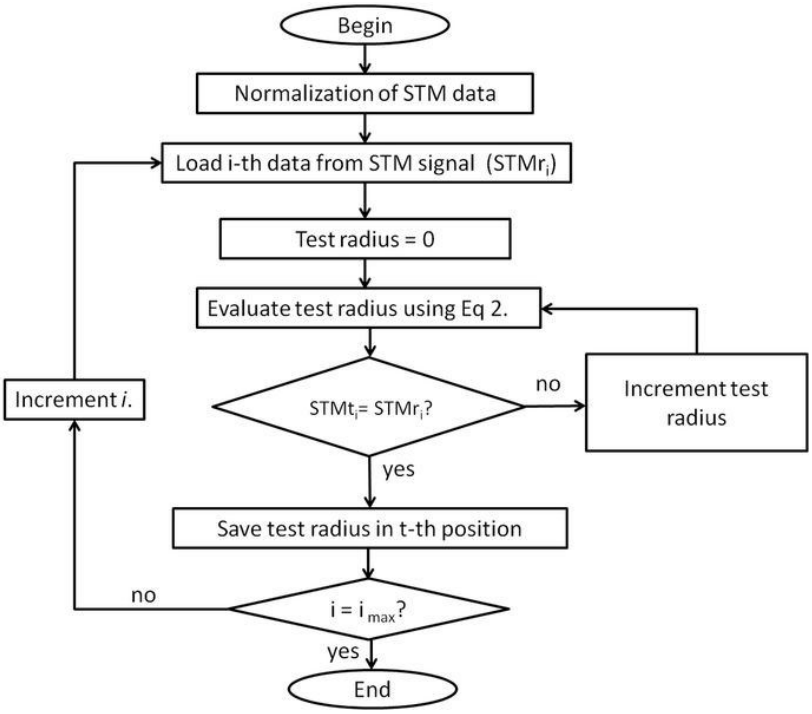

FIG. 7: Flow diagram describing the algorithm to calculate the bubble radius based on the experimentally obtained STM signal.

The first integral in the numerator and that in the denominator have the same value as the first integral of Eq. (2), representing the area of the probe beam. The second integral in the numerator has rp as the limits of integration and represents the portion of the probe beam blocked by a bubble of radius rp. The fourth step compares these two values ($STMt$ and $STMr$), and changes rp incrementally if the two STM values do not match. The cycle is repeated until the rp reaches a value such that the $STMt$ value closely matches the $STMr$ value.

Figure 8 shows a comparison between the bubble radius as a function of time computed from the experimentally obtained STM signal and the bubble radius experimentally obtained using high-speed video. The very good agreement between the simulated bubble dynamics and the video processing results, shown in Fig. 8, was achieved for a He-Ne probe beam radius of 650 μm. The measured $1/e^2$ He-Ne beam radius was 575 μm; however, we must point out that we found that the beam edge has enough light to still record the bubble event.

5. CONCLUSIONS

We have demonstrated a simple and fast experimental technique (STM) together with a simple analytical analysis and an algorithm to compute the pulsed laser-induced bubble dynamics. This technique reduces the uncertainty originated in the high-speed video, laser shadowgraphy and other time-resolved imaging techniques, notably missing the collapses during the cavitation bubble dynamics event. This work presented here also

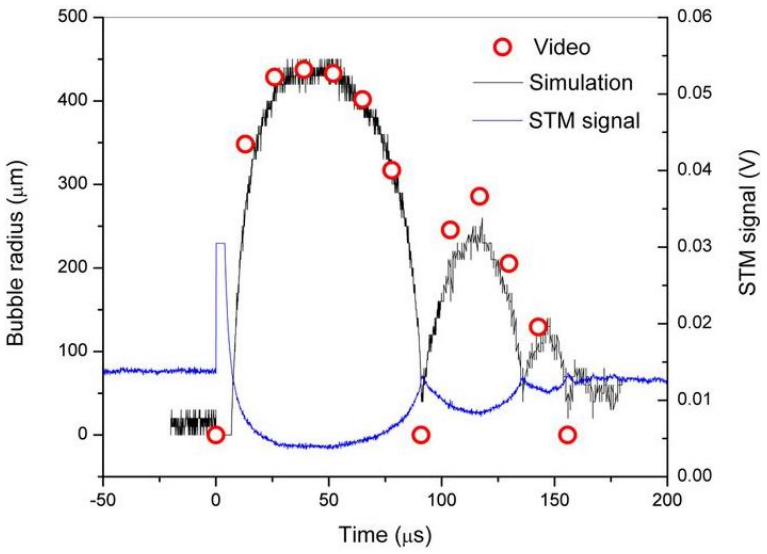

FIG. 8: Comparison between the bubble size extracted from the high-speed video and the computed bubble size from the STM signal presented in this work.

helps to overcome the difficulty of having a repeatable shot-to-shot laser pulse energy when using Q-switched lasers, which is essential for the success if using the time-resolved laser shadowgraphy technique.

ACKNOWLEDGMENTS

This work has been funded by PROMEP support for Apoyo a la Incorporación de Nuevos Profesores de Tiempo Completo (PROMEP/103.5/11/3671). The authors thank both Dr. Enrique Rodríguez-Lara and Dr. Juan Pablo Rodriguez-Pérez for very useful discussions on the ophthalmic applications of this work. The authors also acknowledge partial support for this work from Clínica de Ojos de Tijuana and Oftálmica Internacional through Grant no. F0E017.

REFERENCES

Alehossein, H. and Qin, Z., Numerical analysis of Rayleigh–Plesset equation for cavitating water jets, *Int. J. Numer. Methods Eng*., vol. **72**, no. 7, pp. 780–807, 2007.

Brujan, E. A. and Vogel, A., Stress wave emission and cavitation bubble dynamics by nanosecond optical breakdown in a tissue phantom, *J. Fluid Mech*., vol. **558**, pp. 281–308, 2006.

Devia-Cruz, L., Camacho-López, S., Evans, R., García-Casillas, D., and Stepanov S., Laser-induced cavitation phenomenon studied using three different optically-based approaches—An initial overview of results, *Photonics Lasers Med.*, vol. **1**, no. 3, pp. 143–229, 2012.

Docchio, F., Regondi, P., Capon, M. R., and Mellerio, J., Study of the temporal and spatial dynamics of plasmas induced in liquids by nanosecond Nd:YAG laser pulses. 1: Analysis of the plasma starting times, *Appl. Opt.*, vol. **27**, no. 17, pp. 3661–3668, 1988.

Evans, R., Camacho-López, S., Pérez-Gutiérrez, F. G., and Aguilar, G., Pump-probe imaging of nanosecond laser-induced bubbles in agar gel, *Opt. Express*, vol. **16**, no. 10, pp. 7481–7492, 2008.

Evans, R. and Camacho-López, S., Pump-probe imaging of nanosecond laser-induced bubbles in distilled water solutions: Observations of laser-produced-plasma, *J. Appl. Phys.*, vol. **108**, no. 10, pp. 103106-1–103106-9, 2010.

Gregorčič, P., Petkovšek, R., Možina, J., and Monik, G., Measurements of cavitation bubble dynamics based on a beam-deflection probe, *Appl. Phys. A*., vol. **104**, no. 93, pp. 901–905, 2008.

Kaustubh, R. R., Quinto-Su, P. A., Hellman, A. N., and Venugopalan, V., Pulsed laser microbeam-induced cell lysis: Time-resolved imaging and analysis of hydrodynamic effects, *Biophys. J.*, vol. **91**, no. 1, pp. 317–329, 2006.

Lauterborn, W. and Ohl, C. D., Cavitation bubble dynamics, *Ultrasonics Sonochem.*, vol. **4**, no. 2, pp. 65–75, 1997.

Liu, X.-M., Liu, X.-H., He, J., Hou, Y.-F., Lu, J., and Ni, X.-W., Cavitation bubble dynamics

in liquids of different viscosity, In *Proc. of Symposium on Photonics and Optoelectronics (SOPO)*, pp. 1–4, 2010.

Oraevsky, A. A., Da Silva, L. B., Rubenchik, A. M., Feit, M. D., Glinsky, M. E., Perry, M. D., Mammini, B. M., Small, W., IV, and Stuart, B. C., Plasma mediated ablation of biological tissues with nanosecond-to-femtosecond laser pulses: Relative role of linear and nonlinear absorption, *Selected Topics in Quantum Electronics IEEE*, vol. **2**, no. 4, pp. 801–809, 1996.

Oraevsky, A. A., Jacques, S. L., Boulevard, H., and Tittel, F. K., Mechanism of laser ablation for aqueous under confined-stress conditions media irradiated, *Stress: Int. J. Biol. Stress*, vol. **78**, pp. 1281–1290, 1995.

Pérez-Gutiérrez, F. G., Camacho-López, S., and Aguilar, G., Time-resolved study of the mechanical response of tissue phantoms to nanosecond laser pulses, *J. Biomed. Opt.*, vol. **16**, p. 115001, 2011.

Petkovsek, R., Gregorcic, P., and Mozina, J., A beam-deflection probe as a method for optodynamic measurements of cavitation bubble oscillations, *Meas. Sci. Technol.*, vol. **18**, no. 9, pp. 2972–2978, 2007.

Prentice, P., Cuschieri, A., Dholakia, K., Prausnitz, M., and Campbell, P., Membrane disruption by optically controlled microbubble cavitation, *Nat. Phys.*, vol. **1**, no. 2, pp. 107–110, 2005.

Vogel, A. and Lauterborn, W., Acoustic transient generation by laser-produced cavitation bubbles near solid boundaries, *J. Acoust. Soc. Am.*, vol. **84**, no. 2, pp. 719–731, 1988.

Vogel, A., Lauterborn, W., and Timm, R., Optical and acoustic investigations of the dynamics of laser-produced cavitation bubbles near a solid boundary, *J. Fluid Mech.*, vol. **206**, pp. 299–338, 1989.

Xu, R., Zhao, R., Cui, Y., Lu, J., and Ni, X., Investigation of cavitation bubble dynamics by fiber-coupling optical beam deflection technique, *Microwave Opt. Technol. Lett.*, vol. **50**, no. 7, pp. 1767–1770, 2008.